J Mol Hist
DOI 10.1007/s10735-012-9477-0

ORIGINAL PAPER

Estradiol, progesterone and prolactin modulate mammary gland morphogenesis in adult female plains vizcacha (*Lagostomus maximus*)

Julia Halperin · Veronica B. Dorfman · Nicolas Fraunhoffer · Alfredo D. Vitullo

Received: 22 October 2012 / Accepted: 14 December 2012

Abstract We studied for the first time the mammary gland morphogenesis and its hormonal modulation by immunolocalizing estradiol, progesterone and prolactin receptors (ER, PR and PRLR) in adult females of *Lagostomus maximus,* a caviomorph rodent which shows a pseudo-ovulatory process at mid-gestation. Mammary ductal system of non-pregnant females lacks expression of both ERα and ERβ. Yet throughout pregnancy, ERα and ERβ levels increase as well as the expression of PR. These increments are concomitant with ductal branching and alveolar differentiation. Even though mammary gland morphology is quite similar to that described for other rodents, alveolar proliferation and differentiation are accelerated towards the second half of pregnancy, once pseudo-ovulation had occurred. Moreover, this exponential growth correlates with an increment of both progesterone and estradiol serum-induced pseudo-ovulation. As expected, PR and PRLR are strongly expressed in the alveolar epithelium during pregnancy and lactation. Strikingly, PRLR is also present in ductal epithelia of cycling glands suggesting that prolactin function may not be restricted to its trophic effect on mammary glands of pregnant and lactating females, but it also regulates other physiological processes in mammary glands of non-pregnant animals. In conclusion, this report suggests that pseudo-ovulation at mid-gestation may be associated to *L. maximus* mammary gland growth and differentiation. The rise in progesterone- and estradiol-induced pseudo-ovulation as well as the increased expression of their receptors, all events that correlate with the development of a more elaborated and differentiated ductal network, pinpoint a possible relation between this peculiar physiological event and mammary gland morphogenesis.

Keywords Estradiol · Progesterone · Prolactin · Mammary gland development · Cycling · Pregnancy · Lactation · Involution · Vizcacha · *Lagostomus maximus*

J. Halperin (✉) · V. B. Dorfman · N. Fraunhoffer · A. D. Vitullo
Centro de Estudios Biomédicos, Biotecnológicos, Ambientales y Diagnóstico (CEBBAD), Universidad Maimónides, Hidalgo 775 6to piso, C1405BCK Ciudad Autónoma de Buenos Aires, Argentina
e-mail: halperin.julia@maimonides.edu

J. Halperin · V. B. Dorfman · N. Fraunhoffer · A. D. Vitullo
Consejo Nacional de Investigaciones Científicas y Técnicas (CONICET), Rivadavia 1917, Ciudad Autónoma de Buenos Aires, Argentina

Introduction

The mammary gland is the organ responsible for milk synthesis and secretion and this constitutes the main feature that distinguishes the Mammalian class from the other taxonomic classes in the ranking system. Although it has been proposed a phylogenetic origin from apocrine-like glands that were associated with hair follicles or with sweat glands, the mammary gland is a complex, highly specialized tissue that has evolved to provide nutrition for young offspring (Oftedal 2002). In addition, there are other benefits as the provision of immune factors that are secreted with the milk which have developmental benefits for lactating neonates (McClellan et al. 2008; Hurley and Theil 2011).

The mammary gland is a complex tubulo-alveolar secretory organ formed by epithelial cells that shape the ductal network parenchyma of the gland which is surrounded by connective tissue stroma. Both ducts and

Published online: 26 March 2013

secretory alveoli are lined by a bi-layer epithelium formed by luminal secretory cells surrounded by basal contractile myoepithelial cells. In a mature mammary gland, the structure of the ductal tree is characterized by its basic component which is the milk-secreting alveoli joining up to form groups known as lobules, that group to form lobes, and each lobe has a lactiferous duct that drains into openings in the nipple (Russo and Russo 1987; Vonderhaar 1988). Within the stroma, there are fibroblast, immune cells, vascular endothelial cells, which make up the blood vessels and adipocytes. Stroma does not function as a mere structural support system but it is rather capable of modulating epithelial function through bidirectional modulatory signals to epithelial cells, and vice versa (Schedin and Hovey 2010; Landskroner-Eiger et al. 2010).

Mammary glands are unique compared with the majority of the organs of the body in that the bulk of its development and differentiation occurs in post-natal life (Sakakura 1987). The development of the gland proceeds in distinct phases. During embryonic growth, they develop as a pair of epidermal thickenings called milk lines or mammary ridges. Multiple glands develop into the fat pads located along the ridges which extend from the thoracic to the inguinal region of the animal. In humans, only one pair usually persists, and the ridges disappear elsewhere. From birth until the onset of puberty, mammary glands undergo a period of allometric growth and remain rudimentary shaped as small ducts. After puberty, they rapidly develop under the influence of circulating hormones and growth factors (Brisken and O'Malley 2010 for a review). Ovarian hormones estradiol (E2) and progesterone (P) modulate duct development and branching in cycling virgin animals which leads to the formation of a ductal tree that fills the entire mammary fat pad (Daniel et al. 1987; Russo and Russo 1996; Fendrick et al. 1998). Combined actions of P and prolactin (PRL) induce terminal differentiation of alveolar epithelial cells at the end of gestation with the onset of milk secretion at parturition (Ormandy et al. 1997; Gallego et al. 2001; Brisken 2002). Lack of demand for milk at weaning initiates the process of involution whereby the gland is remodeled back to its pre-pregnancy state (Watson 2006 for a review). Although a large number of studies have indicated the requirement of E2, P and PRL in the development of virgin and mature mammary glands, there is still much to be learned about the roles of these hormones in the development of each of the structural components of this organ.

A significant amount of studies on mammary gland development and physiology have been published in the past two decades (Sternlicht 2006; Mallepell et al. 2006; Watson 2006; Watson and Khaled 2008; Macias and Hinck 2012 for reviews) and they have been specially valuable for researchers and physicians since they contributed to a better understanding of the mechanisms that drive breast cancer in hope to advance in the discovery of therapies to treat this disease. The vast majority of these investigations have been performed on mouse and rat mammary glands. The short generation time, available genetic mutants, and methods for gene modification make these species model organisms for breast cancer research. However, many aspects still remain unfulfilled covered by conventional animal models since these rodents differ considerably in mammary gland development and types of breast cancer from women (Parmar and Cunha 2004; Borowsky 2011). On the other hand, studies performed on unconventional rodents such as guinea pigs and hamsters that share with humans some endocrine and reproductive biology aspects have contributed to a better understanding of human physiology and disease (Keightley and Fuller 1996), particularly on some reproductive tumors (Porter et al. 1995; Liehr 1997).

The South American plains vizcacha, *Lagostomus maximus* is a rodent evolutionary closely related to guinea pig (Jackson et al. 1996) with a seasonal reproductive cycle and nocturnal habits (Fuentes et al. 1991, 1993). Adult females exhibit a gestation period that lasts around 155 days which is unusually long for a rodent (Weir 1971a). This species has attracted significant attention in the reproductive research field since female ovaries exhibit exceptional and unique characteristics among rodents. For instance, they present a natural massive poly-ovulation that can go up to 800 oocytes per cycle, as a result of a strong suppression of apoptosis-dependent follicular atresia (Weir 1971a, b; Jensen et al. 2006, 2008; Leopardo et al. 2011). This particular feature is totally opposed to what is normally found in the developing and mature mammalian ovary (Tingen et al. 2009 for a review). Although at each cycle literally hundreds of eggs are released for fertilization, around 10–12 oocytes successfully fertilize and implant, and two at the most complete their embryonic development (Weir 1971b; Roberts and Weir 1973). Moreover, these animals exhibit a pseudo-ovulation event at mid-pregnancy that leads to an important rise of the progesterone levels (Weir 1971a; Jensen et al. 2006; Dorfman et al. 2011). This additional circulating progesterone may contribute to an accurate maintenance of the uterus and embryo development throughout the end of pregnancy (Jensen et al. 2006; Dorfman et al. 2011) through the addition of a considerable number of secondary corpora lutea (Jensen et al. 2008).

Given the fact that, after the onset of puberty, ovarian hormones modulate growth and development of mammary glands, the reproductive peculiarities of the ovaries of vizcachas make of this species an interesting model to examine mammary gland morphology according to its reproductive state. So far, aside the report published by

Barbara Weir's lab in early 1980s on milk composition (Goode et al. 1981) there have been no further research on *L. maximus* mammary gland development. The aim of this work is to characterize the morphology of the adult mammary gland of *L. maximus* along the reproductive stages: cycling, pregnancy, lactation and involution focusing on the time pseudo-ovulation takes place, and to correlate the glandular development with the expression of reproductive hormone receptors in an attempt to contribute to the understanding of mammary gland hormonal regulation in this peculiar species.

Materials and methods

Animal handling

Forty-nine adult female vizcachas, *L. maximus*, weighting between 1.4 and 3.8 kg were used throughout the present study. Animals were captured using live traps placed in their burrows between June 2011 and June 2012 from a natural population site at the *Estación de Cría de Animales Silvestres*, Province of Buenos Aires, Argentina. In order to establish the different animal groups, vizcachas were captured according to their breeding season: from October to February to obtain non-pregnant animals ($n = 15$); from April to August to find gestating females ($n = 28$) which was established for the presence of implantation sites; and, during September to obtain non-pregnant lactating females ($n = 6$) which was confirmed for the presence of breast milk. Involuting mammary gland group was defined over non-pregnant females captured between October and mid-November and confirmed as such after morphological examination of mammary glands. For the morphological analysis, pregnant animals were divided into early and late pregnants, according to pre and post pseudo-ovulation time, which occurs around mid-June (Weir 1971a; Jensen et al. 2006).

Animals were anesthetized with ketamine 13.5 mg/kg body weight (ketamine clorhydrate, Holliday Scott S.A., Buenos Aires, Argentina) and xilacine 0.6 mg/kg body weight (xilacine clorhydrate, Laboratorios Richmond, Buenos Aires, Argentina) and, after tissue collection they were killed by an intracardiac injection of Euthanyle 0.5 ml/kg body weight (sodium pentobarbital, sodium diphenyl hydantoinate; Brouwer S.A., Buenos Aires, Argentina). All experimental protocols performed in the present study were reviewed and authorized by the Institutional Committee on Use and Care of Experimental Animals of Universidad Maimónides, Argentina. Handling and sacrifice of animals were performed in accordance with all local, state and federal guidelines for the care and utilization of laboratory animals. Husbandry of the animals met the National Institutes of Health Guidelines for the Care and Use of Laboratory Animals (Health Research Extension Act of 1985).

Histology and immunohistochemistry

Mammary glands were surgically extracted and fixed 48 h in cold 4 % paraformaldehyde in 0.01 M phosphate-buffered saline (PBS, pH 7.4), dehydrated through a graded series of ethanol and embedded in paraffin. Each gland was sectioned at 5 μm thick and mounted onto coated slides. Prior to staining, sections were dewaxed in xylene and rehydrated through a decreasing series of ethanol. Morphology was assessed with hematoxylin-eosin and periodic acid-Schiff staining.

Adjacent sections were used for immunohistochemical assays using avidin–biotin-peroxidase complex method. Briefly, sections were dewaxed in xylene and rehydrated through a decreasing series of ethanol, distilled water and PBS, 0.01 M, pH 7.4. Antigen retrieval was performed by boiling sections in 10 mM sodium citrate buffer pH 6 for 20 min. Blocking of peroxidase activity was performed with 2 % hydrogen peroxide in methanol for 30 min. After that, nonspecific binding sites for immunoglobulins were blocked by incubating sections with a blocking solution containing 10 % normal serum of the species in which the primary antibody was made. Immunoreactivity was detected by incubating sections overnight in a moist chamber at 4 °C with the following primary antibodies: anti-ERα rabbit polyclonal IgG, 1:200 dilution (MC-20; sc-542); anti ERβ rabbit polyclonal IgG, 1:200 dilution (H-150; sc-8970); anti-PR rabbit policlonal IgG, 1:200 dilution (C-19, sc-538) and anti-PRLR rabbit polyclonal IgG, 1:200 dilution (H-300, sc 20992) all from Santa Cruz Biotechnology, USA. Specificity controls were performed by omission of the primary antibody and by incubating with a blocking peptide (ERα MC-20P, sc-542P; PR C-19P, sc538P both from Santa Cruz Biotechnology Santa Cruz Biotechnology) and no positive structures or cells were found in these sections.

Section were revealed with a biotinylated goat anti-rabbit IgG followed by incubation with avidin–biotin complex (ABC Vectastain Elite kit, Vector Laboratories, Burlingame, USA). The reaction was visualized with 3,3′ diaminobenzidine (DAB kit, Vector Laboratories, Burlingame, USA). Sections were counterstained with hematoxylin for morphological orientation, dehydrated and mounted. Sections were imaged using an optic microscope (BX40, Olympus Optical Corporation, Tokyo, Japan) fitted with a digital camera (390CU 3.2 Mega Pixel CCD Camera, Micrometrics, Spain), and analyzed using Image Pro Plus software (Image Pro Plus 6, Media Cybernetics Inc, Bethesda Maryland, USA).

Progesterone and estradiol serum determination

After anesthesia, blood samples were taken by cardiac puncture. Blood samples were centrifuged 15 min at 3000 rpm and the serum fraction aliquoted and stored at −80 °C. To determine progesterone (P) and estradiol (E2) serum levels EIAgen Progesterone kit and EIAgen Estradiol kit (Adaltis, Italia) were used according to manufacturer's instructions. Briefly, a direct solid phase enzyme immunoassay detecting a range of 0.18–40.0 ng/ml (0.48–127.2 nmol/l) of P and of 16–2000 pg/ml (59–7340 pmol/l) of E2 were developed. A horseradish peroxidase-labelled hormone competing with P (or E2) present in the serum sample for a fixed limited number of antibody sites immobilized in the wells of the microstrips. The fraction bound to the antibody was measured by adding a chromogen/substrate solution which was converted to a blue compound that changed to yellow with sulphuric acid that stopped the reaction. The absorbance of the solution, photometrically measured at 450 nm, was inversely related to the concentration of P (or E2) present in the sample. Calculation of P and E2 content were made by reference to a calibration curve.

Statistical analysis

Values were expressed as mean ± standard error of the mean. Data were analyzed using one-way analysis of variance and Newman-Keuls multiple comparison post-tests. Differences were considered significant when $P < 0.05$.

Results

General morphology of the mammary gland in mature female vizcachas

Adult female plains vizcachas have two pairs of mammary glands located just below the skin and laterally on the thorax. General morphology of the mature mammary gland is schematized in the top of Fig. 1. The secretory parenchyma of each branched tubulo-alveolar gland is divided into lobes and then lobules by connective tissue septa (Fig. 1A). Lobules are formed by intralobular ducts that connect to an interlobular duct which finally empty into the lactiferous duct (Fig. 1B). The lactiferous duct is the excretory duct of each lobe, and connects to the opening nipple to allow the release of milk during lactation (Fig. 1C). Before reaching the opening nipple, the lactiferous duct lumen forms a lactiferous sinus that functions as a reservoir for milk during lactation (not shown). The openings of the nipple are lined with stratified squamous epithelium, keratinizing variety, which is continuous with that of the skin (Fig. 1C). The ductal orifices contain keratinous cell debris. The lactiferous duct is delimited by a two-layer epithelium that lies on the basement membrane which separates the parenchymal and stromal compartments (Fig. 1D). Surrounding stroma is mainly composed by dense connective tissue, endothelial vessels (Fig. 1A) and immune cells (Fig. 1D). Unlike to what have been described for mouse and rat,adult vizcachas mammary

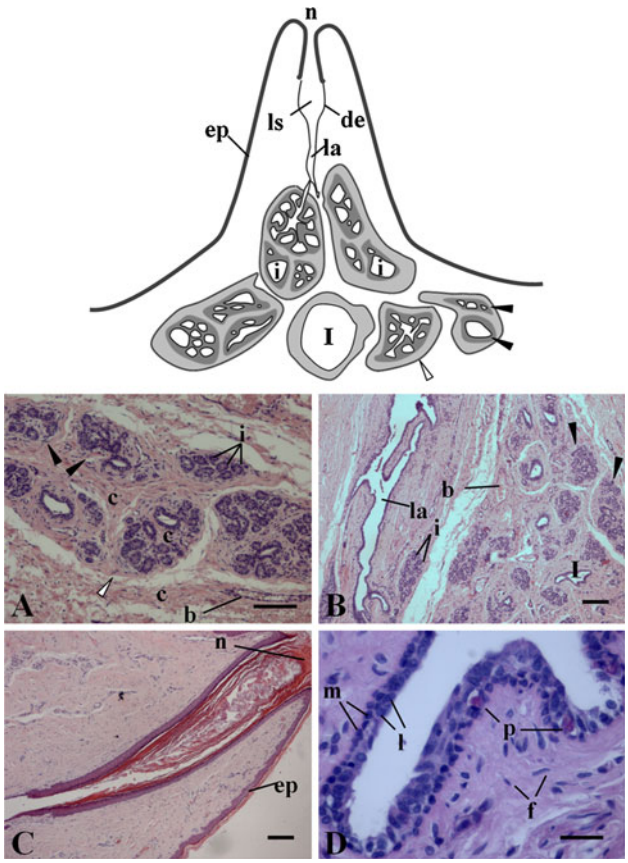

Fig. 1 General morphology of the adult female *Lagostomus maximus* mammary gland. *Top*: Schematic draw depicts the general morphology of an adult female *L. maximus* mammary gland. *Bottom*: Representative photomicrographs of sagital sections of mammary glands of adult female vizcachas. **A** Secretory parenchyma of the mammary gland is composed by intralobular ducts forming lobules that join into lobes. Surrounding stroma is composed by connective tissue. **B** Intralobular ducts empty into an interlobular duct which then will connect with the lactiferous duct. **C** Lactiferous duct epithelium is continuous with the stratified squamous epithelium of the nipple opening which is continuous with skin epidermis. **D** Bi-layered epithelium that lines the ductal network exhibits a luminal secretory cell layer and a basal myoepithelial cell layer and is surrounded by stromal cells. Panels **A**–**C** were stained with hematoxylin-eosin and panel **D** with P.A.S. Scale bar in panel **A** represents 100 μm; in panel **B** and **C** represents 150 μm and in panel **D** represents 25 μm. *Abbreviations*: *b* blood vessel, *c* connective tissue, *de* ductal epithelium, *ep* epidermis, *f* fibroblasts, *i* intralobular duct, *I* interlobular duct, *l* luminal secretory cells, *la* lactiferous duct, *ls* lactiferous sinus, *m* myoepithelial cells, *n* nipple opening, *p* polymorphonuclear cells, *filled arrowhead* lobules, *empty arrowhead* lobe

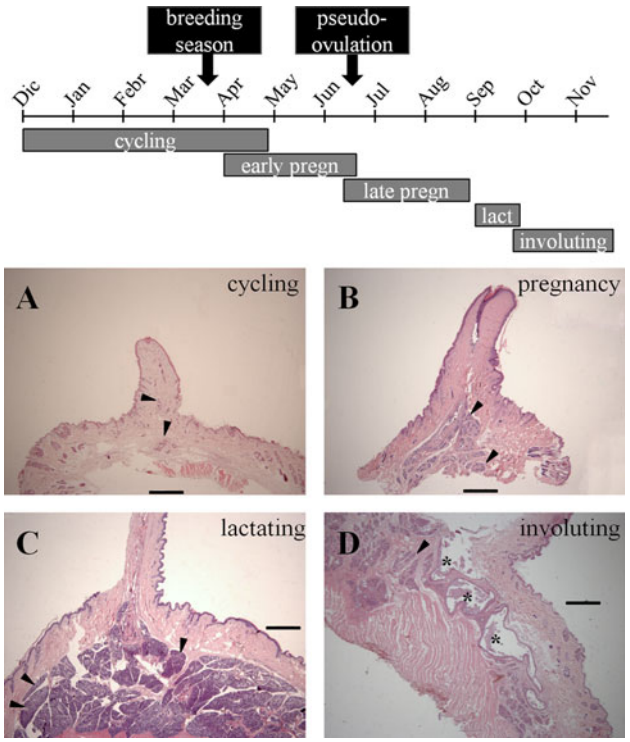

Fig. 2 Mammary gland morphology of the adult female *Lagostomus maximus* according to its reproductive stage. *Top*: Timeline showing capture time points for each adult female group throughout the annual breeding habits and the pseudo-ovulation at mid-gestation. *Bottom*: Representative photomicrographs comparing the general aspect of the mammary gland morphology of adult female vizcachas along the distinct reproductive stages. **A** Mammary gland of a cycling female present a rudimentary ductal network formed by interlobular ducts surrounded by dense connective tissue. **B** Mammary gland of a pregnant female exhibit high proliferation and branching of the ductal network which is evidenced by a marked increase in the lobule number. **C** Mammary gland parenchyma of lactating females is almost completely occupied by milk-secreting alveoli. **D** Mammary gland going through a process of involution exhibits its parenchymal structure disorganized, the interlobular ducts with milk remains and reorganization of the connective tissue. *Panels* **A–D** were stained with hematoxylin-eosin. *Scale bar* in panels **A–D** represents 100 μm. *Filled arrowhead* Lobules,* milk remains

glands have a poor fat content in the fat pad which is the main reason why whole mounting analysis could not be performed. The extent of the development of the ductal network depends on whether the animal is cycling, pregnant, lactating or in a post weaning period (Figs. 2, 3).

Cycling females

Short before breeding season, mammary glands of non-pregnant adult females are in a "resting" state and present predominance of stromal connective tissue over the rudimentary ductal tree which is mainly characterized by few ducts and scarce secretory alveoli (Figs. 2A, 3A–C). Quiescent glandular lobules are surrounded by dense interlobular connective tissue. Both ducts and alveoli are lined by a two layered epithelium composed by an inner layer of cuboidal luminal secretory cells surrounded by basal contractile myoepithelial cells. Although at this stage, there is no secretory activity, some ducts may show content in their lumen.

Pregnancy

Throughout pregnancy, the mammary gland of female vizcachas exhibits structural changes in preparation for lactation of progeny (Figs. 2B, 3D–I). A qualitative examination based on the morphological analysis shows that the glandular parenchyma to stroma ratio starts to increase as well as the vascularization within the connective tissue that surrounds each lobule (Fig. 3D). During the first half of pregnancy, which extends from begining of April to mid/June (Fig. 2, top), there is an increase in branching and elongation of the ductal tree. Bulbous terminal end buds (TBEs) formed at the tip of growing ducts during ductal morphogenesis (not shown), now proliferate and bifurcate generating new branches (Fig. 3E, F). TEBs show multiple layers of epithelium implying a high proliferative rate of this cell population (Fig. 3F).

At late pregnancy (mid-June to begining of September, Fig. 2, top), the alveolar buds located at the end of the branches progressively cleave and differentiate into individual alveoli which occupy the majority of the fat pad (Fig. 3G–I). Right before parturition, alveolar epithelial cells are enlarged due to high cytoplasmic lipid content. These alveoli will ultimately become milk-secreting lobules during lactation. Presence of proteins in the lumen can be evidenced by a purple/pink staining in hematoxilin-eosin sections.

Lactation

In mammary glands of lactating animals, milk-secreting alveoli occupy most of the lobule (Figs. 2C, 3J–L). Secretory epithelial cells are cuboidal and visibly polarized. Nucleus is positioned basally and the cytoplasm is vacuolated and full of milk droplets. Lumen of alveoli and ducts are full of milk as well (Fig. 3K, L). Contraction of myoepithelial cells that surrounds alveoli helps to empty their content. Interlobular duct collects the milk released by secretory alveoli (Fig. 3K). A very thin connective tissue sheath surrounds each alveolus (Fig. 3L). Immune cells are present in the stromal connective tissue and within the milk present in the alveoli and ducts lumen (Fig. 3L).

No differences were observed in the morphology between anterior and posterior mammary glands. Anterior as well as posterior glands are highly branched and full of milk. Lactating females exhibit only one milk patch

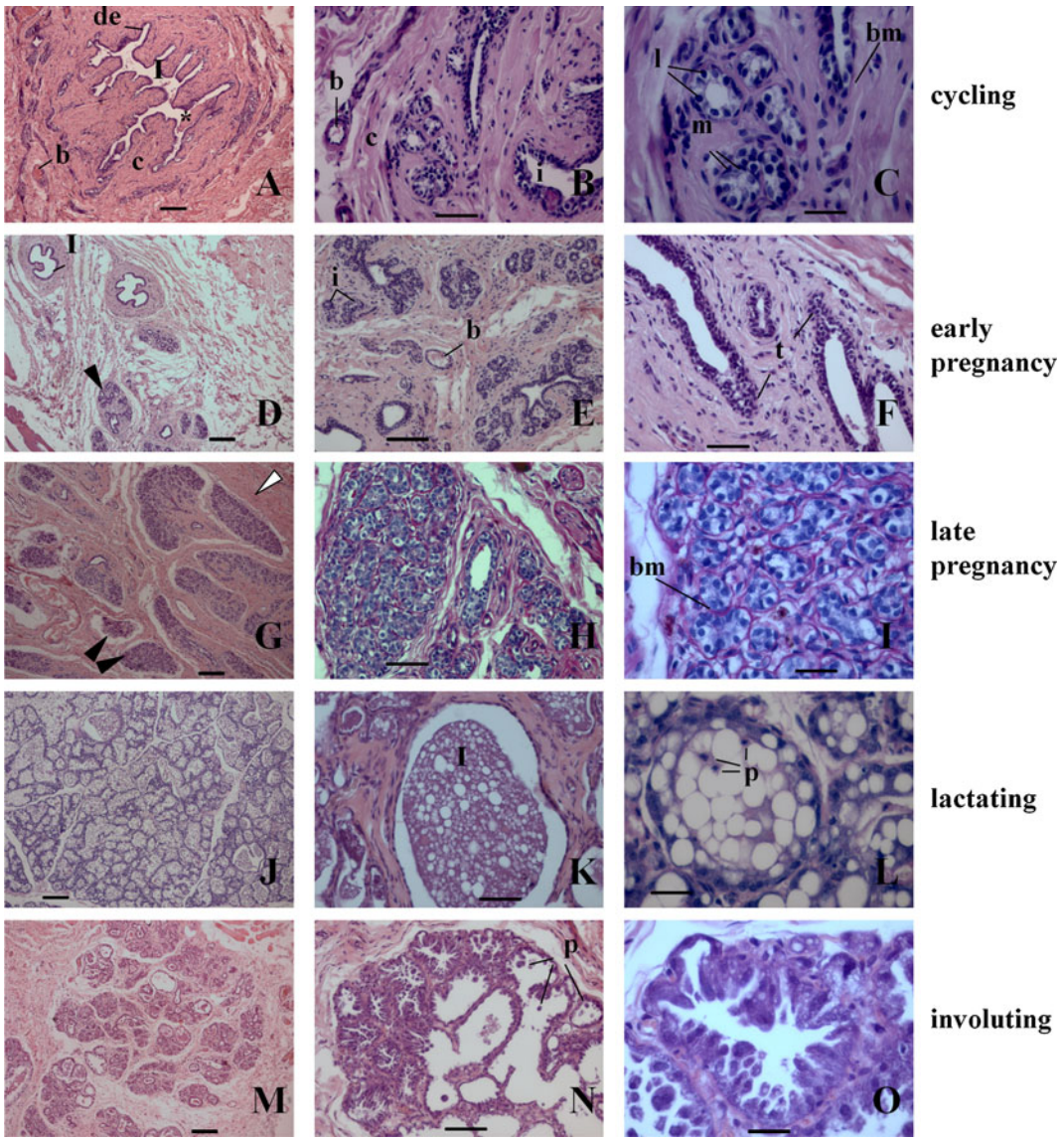

Fig. 3 Representative photomicrographs comparing cellular architecture within the mammary gland of adult female vizcachas along the distinct reproductive stages. **A** Glandular parenchyma of cycling females is composed by interlobular ducts, scarce alveoli and it is surrounded by connective tissue. **B** The inactive duct system of a cycling female is depicted at higher magnification. **C** Bi-layered epithelium that lines ducts and alveoli is composed by luminal secretory cells and basal myoepithelial cells and it rests on a basement membrane that divides parenchymal and stromal compartments. **D** During early pregnancy, as the secretory ducts begin to sprout, the parenchyma: stroma ratio of the gland starts to increase. **E** Mammary gland of a pregnant female exhibit ductal extension, side-branching and lobuloalveolar development. **F** At pregnancy, TBEs formed at the tip of growing ducts proliferate and bifurcate generating new branches. TEBs show multiple cell layers implying a high proliferative rate. **G** At late pregnancy, the stromal connective tissue further recedes and the gland parenchyma increases. Alveolar buds progressively cleave and differentiate into individual alveoli. **H** During alveolar morphogenesis, epithelial cell number increases as well as the epithelial surface within each lobule. **I** Alveolar secretory cells become a sphere-like layer of enlarged and polarized cells that envelops a circular lumen. Alveolar cells hypertrophy and accumulate milk fat droplets. **J** Mammary glands of lactating females show milk-secreting alveoli in their maximum level of differentiation and occupying most of the lobular space giving a spongy appearance. **K** Interlobular duct collecting the milk drained from the lobules. **L** Alveolar secretory cells exhibit their cytoplasm full of milk droplets. The apical cell membrane may rupture and milk fat droplets are pinched off as apical protrusions. These attributes are characteristic of apocrine glands. **M** After weaning, mammary gland parenchyma exhibits disorganization of the lobular structure. **N** During involution, alveoli start to collapse, basement membrane becomes fragmented and connective tissue starts to refill. Abundant polymorphonuclear cells are recruited. **O** Detachment of alveolar epithelial cells that shed into the lumen is a characteristic feature of this stage. Panels **A**, **D**, **E**, **G**, **J**–**N** were stained with hematoxylin-eosin and **B**, **C**, **F**, **H**, **I** and **O** with P.A.S. *Scale bar* in *panels***A**, **D**, **G**, **J** and **M** represent 150 μm: in *panel***E** represents 100 μm; in panels **B**, **F**, **H**, **K** and **N** represent 50 μm and in panels **C**, **I**, **L** and **O** represent 25 μm. *Abbreviations*: *b* blood vessel, *c* connective tissue, *bm* basal membrane, *de* ductal epithelium, *i* intralobular duct, *I* interlobular duct, *l* luminal secretory cells, *m* myoepithelial cells, *n* nipple opening, *p* polymorphonuclear cells, *t* terminal end buds, *filled arrowhead* lobules, *empty arrowhead* lobe, * milk remains

beneath the skin along the milk line that contains both anterior and posterior nipples.

Involution

Weaning of the litter triggers the process of involution whereby the mammary gland is remodeled back to its prepregnancy state (Figs. 2D, 3M–O). One of the initial signs that characterized this stage is the detachment of alveolar epithelial cells that shed into the lumen (Fig. 3N, O). The structure of the gland display major changes: alveloli start to collapse, basement membrane becomes fragmented and connective tissue, mostly fibroblast and some adipocytes, start to refill. It is notorious the presence of polymorphonuclear cells with their characteristic threelobed nuclei, in the stroma, infiltrated in the secretory epithelia and in the lumen of the alveoli and ducts (Fig. 3N, O).

These mechanisms that ultimately lead to involution of the gland are not synchronized in the entirety of the gland. Whereas some lobules display their ductal network disorganized and massive epithelial cell death, other lobules still show alveolar epithelial cells with cytoplasmic fat droplets and alveoli and intralobular ducts with milk remains.

Immunohistochemistry for ERα, ERβ, PR and PRLR

ERα expression

Immunoexpression of ERα is almost absent in mammary glands of adult cycling females (Fig. 4A). However, during pregnancy ERα markedly increases its expression in the nuclei of stromal cells located beneath the epithelial ducts and alveoli. (Fig. 4B). ERα reaches its maximum level of immunoreactivity during gestation. After parturition, immunoexpression level in mammary glands of lactating females is not strong as in pregnancy, yet few positive cells are still present in the thin sheath of stroma that surrounds milk-secreting alveoli (Fig. 4C). Finally, all ERα expression disappears when the gland starts its involution (Fig. 4D).

ERβ expression

Conversely to ERα, ERβ immunoexpression is very mild in the stroma but it is distinctly present in the cytoplasm of secretory epithelial cells. ERβ staining is weak in mammary glands of non-pregnant females (Fig. 5A). However, during pregnancy the level of immunoreactivity markedly increases in the cytoplasm of alveoli and of ducts as well. Maximal level of immunoexpression for this steroid receptor in the mammary gland occurs at this stage (Fig. 5B). During lactation, ERβ expression declines but is still noticeable in the cytoplasm of milk-producing alveoli and such expression is maintained through the first phase of mammary gland involution, which can be evidenced in the shedding secretory alveolar cells (Fig. 5C, D).

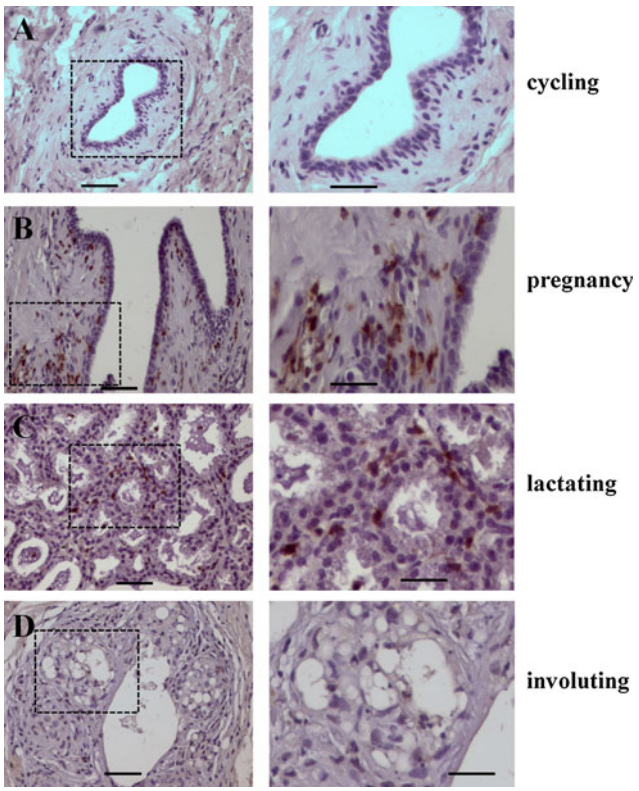

Fig. 4 Representative photomicrographs of mammary gland sections of adult female vizcachas along the distinct reproductive stages immunostained for estrogen receptor α (ERα). **A** Mammary gland of a cycling female shown absence of ERα. **B** During pregnancy, stromal cells located beneath epithelial ducts exhibit nuclear ERα immunoexpression. Maximal level of immunoreactivity occurs during this stage. Secretory parenchyma does not express this steroid receptor. **C** During lactation some stromal cells still express ERα. **D** ERα expression disappears when the mammary gland starts its involution. **A**–**D** Immunoreactivity is shown is *brown* and hematoxylin-counterstained nuclei in *blue*. *Right panels* are detailed views of the *dashed frames* depicted on the corresponding *left panel*. *Scale bar* in the *left panels* represent 50 μm whereas in the *right panel* represent 25 μm

PR expression

PR display a singular pattern of immunoexpression in mammary glands: cycling and pregnant females express PR in the nuclei of TBEs cells as well as in alveolar bud cells (Fig. 6A, B). PR immunoreactivity positively correlates with the degree of branching and development observed in the histological examination (Fig. 2). Interestingly, during lactation, PR expression is noticeable stronger and it partially shifts to the cytoplasm of alveolar cells although some nuclei still show positivity for this receptor (Fig. 6C). Lactation is the stage where maximal

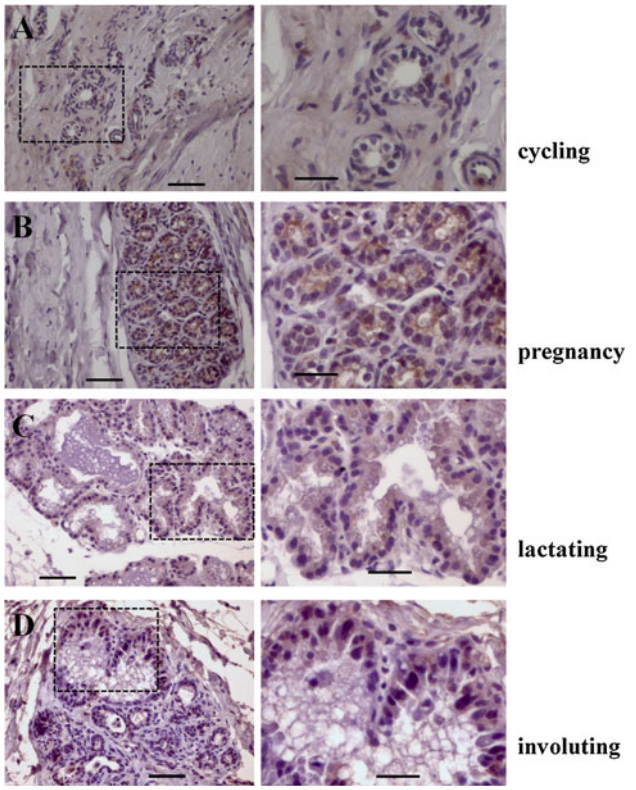

Fig. 5 Representative photomicrographs of mammary gland sections of adult female vizcachas along the distinct reproductive stages immunostained for estrogen receptor β (ERβ). **A** Immunolocalization of ERβ is weak in mammary glands of cycling females. **B** During pregnancy, ERβ localizes in the cytoplasm of ducts and alveoli. Maximal level of immunoreactivity occurs during this stage. Stromal cells do not show positivity for this steroid receptor. **C** During lactation, ERβ continue to localize in the cytoplasm of alveolar secretory cells. **D** ERβ immunolacalization remains in cytoplasm of alveolar cells through the first phase of mammary gland involution. **A–D** Immunoreactivity is shown is *brown* and hematoxylin-counterstained nuclei in *blue*. *Right panels* are detailed views of the *dashed frames* depicted on the corresponding *left panel*. *Scale bar* in the *left panels* represent 50 μm whereas in the *right panel* represent 25 μm

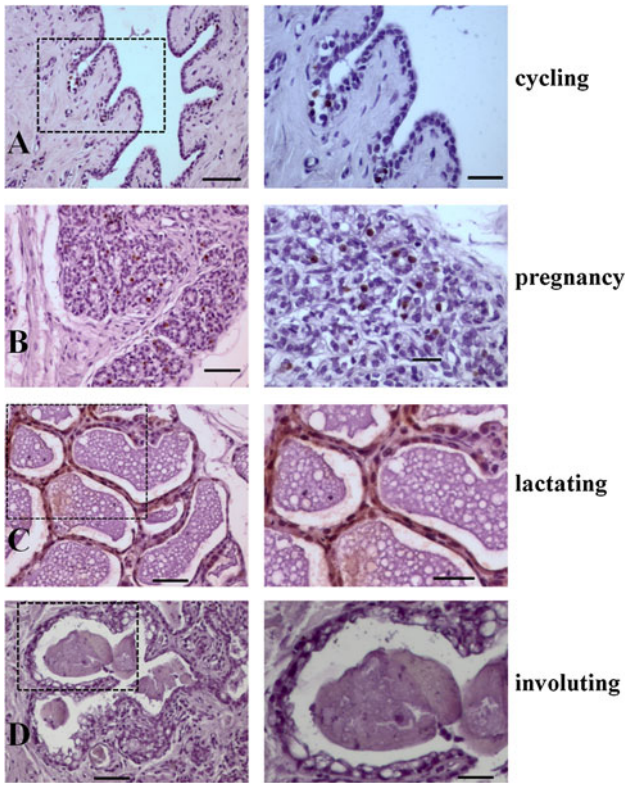

Fig. 6 Representative photomicrographs of mammary gland sections of adult female vizcachas along the distinct reproductive stages immunostained for progesterone receptor (PR). **A** PR localizes in some nuclei of the epithelial ducts of cycling females. **B** During pregnancy, as the ductal system proliferates and branches, PR immunoreactivity markedly increases. Stromal cells do not show positivity for this steroid receptor. **C** During lactation, PR expression becomes stronger and it partially shifts to the cytoplasm of alveolar cells. Lactation is the stage where maximal immunoreactivity of PR is observed. **D** When the gland is involuting, PR expression is suppressed. **A–D** Immunoreactivity is shown is *brown* and hematoxylin-counterstained nuclei in *blue*. *Right panels* are detailed views of the *dashed frames* depicted on the corresponding *left panel*. *Scale bar* in the *left panels* represent 50 μm whereas in the *right panel* represent 25 μm

immunoreactivity of PR is observed. When the gland is involuting, PR expression is suppressed (Fig. 6D).

PRLR expression

As a transmembrane protein, immune-detection of PRLR expression shows cytoplasmic membrane positivity; yet, some nuclei are positive as well (Fig. 7A–D). PRLR immunoreactivity increases as pregnancy progresses and the staining is mainly visualized in the epithelium; however, there are some stromal cells that express PRLR as well (Fig. 7B). Among the analyzed developmental stages, the strongest PRLR immunoreactivity is visualized in mammary glands of lactating females, essentially in the cytoplasm of milk secreting alveoli (Fig. 7C). Likewise PR, PRLR expression ceases during involution of mammary gland (Fig. 7D). Surprisingly, mammary glands of cycling non-pregnant females also express PRLR. This expression localizes mainly in the epithelia that lines the glandular ducts and in some cells of the surrounding connective tissue (Fig. 7A).

Estradiol and progesterone serum levels in relation to the reproductive stage

Estradiol (E2) serum levels showed remarkable variations among the analyzed groups ($P < 0.0001$). Before breeding season, non-pregnant (cycling) female vizcachas have 25.9 ± 5.4 pg/ml of circulating E2 ($n = 7$) and this hormone level is maintained with almost no variations during early pregnancy (24.32 ± 2.0 pg/ml, $n = 10$). However,

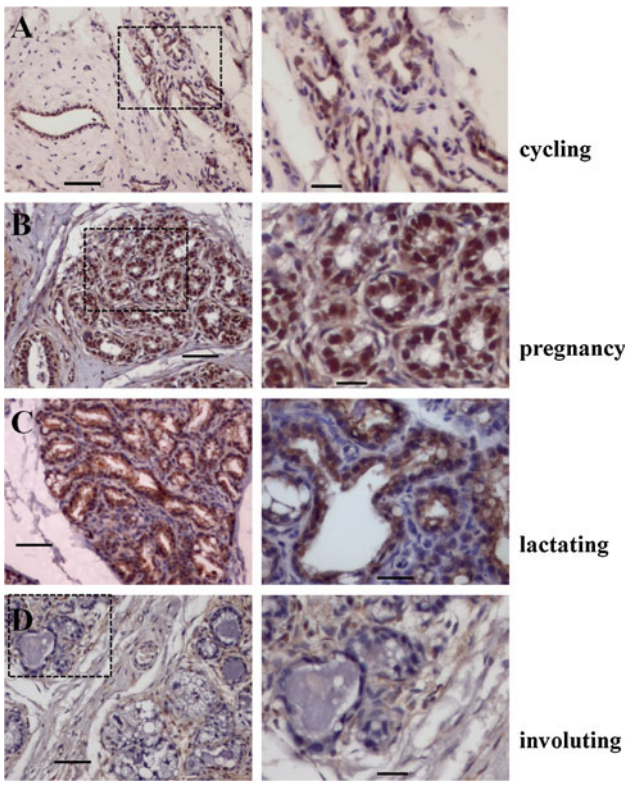

Fig. 7 Representative photomicrographs of mammary gland sections of adult female vizcachas along the distinct reproductive stages immunostained for prolactin receptor (PRLR). **A** PRLR localizes in both nucleus and cytoplasm of the epithelial ducts of cycling females. Stromal tissue does not show positivity for this receptor. **B** PRLR immunoreactivity markedly increases during pregnancy and such expression localizes in both nuclear and cytoplasmic compartments. **C** During lactation, PRLR positive staining becomes stronger and it specifically localizes in the cytoplasm of alveolar cells. Lactation is the stage where maximal immunoreactivity of PRLR is observed. **D** When the gland is involuting, PRLR expression noticeably diminishes. **A–D** Immunoreactivity is shown is *brown* and hematoxylin-counterstained nuclei in *blue*. *Right panels* are detailed views of the *dashed frames* depicted on the corresponding *left panel*. *Scale bar* in the *left panels* represent 50 μm whereas in the *right panel* represent 25 μm

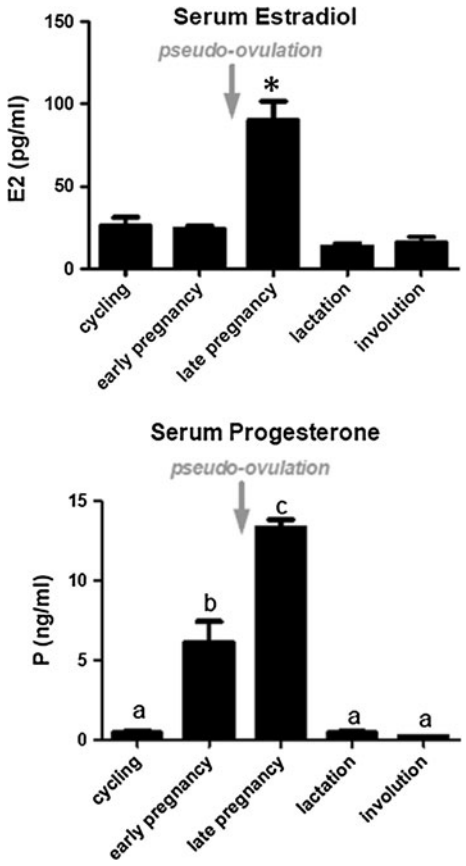

Fig. 8 Measurements of estradiol and progesterone plasma levels along the distinct reproductive stages of adult female vizcachas. *Top*: statistical analysis of circulating estradiol (E2) shows an increment of more than threefold after pseudo-ovulation at mid-gestation compared to E2 serum levels of cycling females. After parturition, E2 values drop close to pre-pregnancy levels ($P < 0.0001$). *Bottom*: progesterone (P) increases its serum concentration more than tenfold during early pregnancy and continued to significantly rise after pseudo-ovulation at mid-pregnancy reaching almost a 30-fold augment compared to P serum levels of cycling females. As expected, circulating P level dropped dramatically after parturition and it kept low during lactation and involution of the mammary gland, being theses values close to pre-pregnancy values ($P < 0.0001$)

once pseudo-ovulation took place at mid-pregnancy (Weir 1971a, b; Jensen et al. 2006) circulating E2 rise significantly to 90.19 ± 11.46 pg/ml (n = 18) and then, after parturition, it abruptly declines to 13.41 ± 1.81 pg/ml during lactation (n = 5). During involution of mammary gland serum E2 values are kept low (15.82 ± 3.45 pg/ml, n = 8) (Fig. 8).

Progesterone (P) serum levels showed striking variations among the studied groups as well ($P < 0.0001$). Whereas cycling females showed very low P serum values (0.45 ± 0.14 ng/ml, n = 9), this level increased more than tenfold during early pregnancy (6.13 ± 1.32 ng/ml, n = 12) and continued to rise after pseudo-ovulation at mid-pregnancy (13.32 ng/ml, n = 8) reaching an almost 30-fold increment compared to cycling (non-pregnant) females mean values. As expected, circulating P level dropped dramatically after parturition and it kept low during lactation (0.46 ± 0.1 ng/ml, n = 5) and after weaning of the litter, when the gland started the process of involution (0.23 ± 0.01 ng/ml, n = 4).

Discussion

We here describe for the first time the mammary gland morphology of adult female of *Lagostomus maximus* along the reproductive stages: cycling, pregnancy, lactation and involution. We show that cycling vizcachas exhibit a simple ductal network lined by a luminal secretory epithelial layer

that rests on a basement myoepithelial cell layer. Surrounding stroma is formed mainly by dense connective tissue, fibroblasts, endothelial cells, immune cells and scarce adipocytes. As females transit throughout pregnancy and lactation, the mammary gland develops a more elaborated structure as a result of proliferation, branching and differentiation of the ductal tree. Particularly along pregnancy, mammary ductal network becomes noticeably more ramified after pseudo-ovulation had occurred. During lactation, mammary gland is almost completely occupied by milk secreting alveoli. It has been previously reported that litter suckling activity of plains vizcachas is confined to the anterior pair (Goode et al. 1981). However we observed that at the end of pregnancy and during lactation all four glands produce milk. Moreover, litter suckling occurs indistinctly among the nipples which appear from the teeth wounds observed in all four nipples. After weaning, mammary glands return to a prepregnancy state in a process that involves polymorphonuclear cell recruitment, alveolar disorganization and cell death.

In contrast to most rodents, females of South American plains vizcachas show a unique ovarian endocrinology characterized by natural massive polyovulation, strong suppression of apoptosis-dependent follicular atresia, pseudo-ovulation during pregnancy together with a singular reproductive hormones profile (Weir 1971a, b; Jensen et al. 2006, 2008; Leopardo et al. 2011; Dorfman et al. 2011). These unusual reproductive aspects suggest a particular hormonal modulation of mammary gland development.

Female reproductive hormones E2, P and PRL are master regulators of mammary gland postnatal development (Nandi 1958; Lyons 1958). Even though mammary gland morphology of adult females' vizcachas is quite similar to that described in other rodents (Richert et al. 2000), our data on E2 and P serum levels as well as the expression of their receptors along the distinct mammary gland reproductive stages suggest a singular hormonal regulation of growth and development of the mammary gland. As opposed to what have been previously reported for virgin mouse mammary glands (Bocchinfuso et al. 2000; Mallepell et al. 2006; Cheng et al. 2004), our ER immunostaining showed that resting mammary glands of non-pregnant cycling vizcachas have no expression of both E2 receptors (ERα and ERβ). Nonetheless, our group of cycling vizcachas is composed by adult females captured in their natural environment, which have probably experienced one or more previous pregnancy-lactation-involution cycles. Therefore, their mammary glands are not pubertal but they are already mature and their ductal network, even in a "resting" status, already comprise ERα dependent-secondary branching. This may explains the absence of ERα expression in the cycling animals. Nevertheless, our results leave open the question on whether virgin vizcachas exhibit similar expression of ERα and ERß than the reported for other rodents.

Besides its role in pubertal branching, ERα has also shown to be essential in alveologenesis during pregnancy and lactation (Feng et al. 2007). As for ERβ, it has been reported its requirement for normal lobuloalveolar development during pregnancy rather than for prepubertal growth (Förster et al. 2002). Our data shows that, once pseudo-ovulation had occurred at mid-pregnancy, circulating E2 reaches its maximal level and both ERα and ERβ immunoexpression peak. More interestingly, these facts correlate with the accelerated ductal proliferation, branching and alveolar differentiation observed during the histological examination of mammary glands of pregnant females.

As a major regulator of postnatal mammary gland development, E2 was thought to exert its effects through ER expressed in the mammary gland stroma and epithelium. By grafting ERα-/- epithelium or stroma in combination with ERα WT stroma or epithelium, Mallepell et al. (2006) have shown that both before and during pregnancy, the primary target for estradiol is the mammary epithelium whereas a direct response of the mammary stroma is not required for mammary gland development to proceed normally. To our surprise, in mammary glands of pregnant vizcachas, ERα localizes in nuclei of stromal cells located immediately beneath the secretory epithelium. Yet, it still supports the idea of a paracrine role for this transcription factor (Mallepell et al. 2006). As for ERβ, it is present mainly in the cytoplasm of ductal epithelial cells (Palmieri et al. 2004). Nevertheless, further quantitative assays should be performed to support our qualitative immunohistochemistry data.

Our results on PR immunoexpression among the distinct reproductive stages are in agreement to what have been described in mammary gland of other rodents (Macias and Hinck 2012). PR is expressed at all times in mammary glands of adult *L. maximus*, except when the gland is involuting. A qualitative interpretation based on the immunohistochemistry analysis indicates that the level of expression positively correlates with the degree of ductal network proliferation and differentiation. Prior to parturition PR localizes in the nuclei of TBE cells and alveolar buds (Fig. 6A, B). Given the fact that proliferation and branching occur mainly from mitosis of TEB cells (Sternlicht 2006), our data strongly supports the autocrine proliferative role described for this receptor on pregnancy-associated ductal side-branching and lobuloalveolar development (Mulac-Jericevic et al. 2003). Interestingly, during lactation there is a partial shift to the cytoplasm of milk-secreting alveoli. This could indicate that our PR antibody recognizes both isoforms of PR (PRA and PRB) which have been described co-expressing in mice mammary gland at late pregnancy (Shyamala et al. 2000). As expected, P serum level augments significantly with pregnancy due to the presence of massive corpora lutea-dependent massive

poly-ovulation. Remarkably, P level increases even further after pseudo-ovulation at mid-gestation.

Finally, PRLR is strongly expressed in alveoli secretory cells during pregnancy and lactation which is in accordance with its well described function in inducing alveologenesis and differentiation into milk-producing cells (Brisken et al. 1999). Interestingly, during pregnancy, part of the PRLR immunoexpression is localized in the cytoplasmic membrane but the nuclear compartment shows a strong immunopositivity as well. It has been proposed that polypeptide ligands like PRL and their receptors may translocate into the nucleus and regulate the expression of specific transcription factors (Clevenger 2003). Although the possibility of an intranuclear function of PRLR in mammary glands of cycling females is novel and intriguing, it exceeds the purpose of this work and it should be subject of future investigations.

Surprisingly, luminal epithelial cells of resting mammary glands of cycling (non-pregnant) vizcachas exhibit a significant level of PRLR expression as well. This data rise the question whether PRL plays a distinct function during this reproductive stage.

Our results suggest that the pseudo-ovulation event that takes place at mid-gestation in *L. maximus* could be associated to mammary gland growth and differentiation. Although other rodents, such as mice and rats, show an accelarated mammary gland development towards the end of gestation, plains vizcachas also exhibit a rise in circulating P- and E2-induced pseudo-ovulation as well as an augment in the expression of their receptors. These events that correlate with the development of a more elaborated and differentiated ductal network, pinpoint a possible relation between this peculiar physiological event and the mammary gland branching and alveolar differentiation. The report presented here opens an avenue for future studies to elucidate the precise contribution of PR, ERα, ERβ, PRLR and other growth factors in mammary gland morphogenesis of South American plains vizcacha.

Acknowledgments This work was supported by a PIP No 0272—CONICET (JH) and by Fundación Científica Felipe Fiorellino, Universidad Maimónides Argentina Intramural Funding. Authors are especially grateful to the personnel of E.C.A.S. for their invaluable help in trapping and handling the animals, and Ms. Grisel Melo for her technical assistance in tissue processing.

References

Bocchinfuso WP, Lindzey JK, Hewitt SC, Clark JA, Myers PH, Cooper R, Korach KS (2000) Induction of mammary gland development in estrogen receptor-alpha knockout mice. Endocrinology 141:2982–2994

Borowsky AD (2011) Choosing a mouse model: experimental biology in context–the utility and limitations of mouse models of breast cancer. Cold Spring Harb Perspect Biol 3:a009670. doi:10.1101/cshperspect.a009670

Brisken C (2002) Hormonal control of alveolar development and its implications for breast carcinogenesis. J MammaryGland Biol Neoplasia 7:39–48

Brisken C, O'Malley B (2010) Hormone action in the mammary gland. Cold Spring Harb Perspect Biol 2:a003178. doi:10.1101/cshperspect.a003178

Brisken C, Kaur S, Chavarria TE, Binart N, Sutherland RL, Weinberg RA, Kelly PA, Ormandy CJ (1999) Prolactin controls mammary gland development via direct and indirect mechanisms. Dev Biol 210:96–106

Cheng G, Weihua Z, Warner M, Gustafsson JA (2004) Estrogen receptors ER alpha and ER beta in proliferation in the rodent mammary gland. Proc Natl Acad Sci USA 101:3739–3746

Clevenger CV (2003) Nuclear localization and function of polypeptide ligands and their receptors: a new paradigm for hormone specificity within the mammary gland? Breast Cancer Res 5:181–187

Daniel CW, Silberstein GB, Strickland P (1987) Direct action of 17 beta-estradiol on mouse mammary ducts analyzed by sustained release implants and steroid autoradiography. Cancer Res 47:6052–6057

Dorfman VB, Fraunhoffer N, Inserra PI, Loidl CF, Vitullo AD (2011) Histological characterization of gonadotropin-releasing hormone (GnRH) in the hypothalamus of the South American plains vizcacha (*Lagostomus maximus*). J Mol Histol 42:311–321

Fendrick JL, Raafat AM, Haslam SZ (1998) Mammary gland growth and development from the postnatal period to postmenopause: ovarian steroid receptor ontogeny and regulation in the mouse. J Mammary Gland Biol Neoplasia 3:7–22

Feng Y, Manka D, Wagner KU, Khan SA (2007) Estrogen receptor-α expression in the mammary epithelium is required for ductal and alveolar morphogenesis in mice. Proc Natl Acad Sci USA 104:14718–14723

Förster C, Mäkela S, Wärri A, Kietz S, Becker D, Hultenby K, Warner M, Gustafsson JA (2002) Involvement of estrogen receptor beta in terminal differentiation of mammary gland epithelium. Proc Natl Acad Sci USA 99:15578–15583

Fuentes L, Caravaca N, Pelzer L, Scardapane L, Piezzi RS, Guzmán J (1991) Seasonal variations in the testis and epididymis of viscacha (*Lagostomus maximus maximus*). Biol Reprod 45:493–497

Fuentes L, Calvo JC, Charreau E, Guzmán J (1993) Seasonal variations in testicular LH, FSH, and PRL receptors; in vitro testosterone production; and serum testosterone concentration in adult male viscacha (*Lagostomus maximus maximus*). Gen Comp Endocrinol 90:133–141

Gallego MI, Binart N, Robinson GW, Okagaki R, Coschigano KT, Perry J, Kopchick JJ, Oka T, Kelly PA, Hennighausen L (2001) Prolactin, growth hormone, and epidermal growth factor activate Stat5 in different compartments of mammary tissue and exert different and overlapping developmental effects. Dev Biol 229:163–175

Goode JA, Peaker M, Weir BJ (1981) Milk composition in the plains viscacha (*Lagostomus maximus*). J Reprod Fertil 62:563–566

Hurley WL, Theil PK (2011) Perspectives on immunoglobulins in colostrum and milk. Nutrients 3:442–474

Jackson JE, Branch LC, Villarreal D (1996) Lagostomus maximus. Mammalian Species 543:1–6. doi:10.2307/3504168

Jensen F, Willis MA, Albamonte MS, Espinosa MB, Vitullo AD (2006) Naturally suppressed apoptosis prevents follicular atresia and oocyte reserve decline in the adult ovary of *Lagostomus maximus* (Rodentia, Caviomorpha). Reproduction 132:301–308

Jensen F, Willis MA, Leopardo NP, Espinosa MB, Vitullo AD (2008) The ovary of the gestating South American plains vizcacha (*Lagostomus maximus*): suppressed apoptosis and corpora lutea persistence. Biol Reprod 79:240–246

Keightley MC, Fuller PJ (1996) Anomalies in the endocrine axes of the guinea pig: relevance to human physiology and disease. Endocr Rev 17:30–44

Landskroner-Eiger S, Park J, Israel D, Pollard JW, Scherer PE (2010) Morphogenesis of the developing mammary gland: stage-dependent impact of adipocytes. Dev Biol 344:968–978

Leopardo NP, Jensen F, Willis MA, Espinosa MB, Vitullo AD (2011) The developing ovary of the South American plains vizcacha, *Lagostomus maximus* (Mammalia, Rodentia): massive proliferation with no sign of apoptosis-mediated germ cell attrition. Reproduction 141:633–641

Liehr JG (1997) Hormone-associated cancer: mechanistic similarities between human breast cancer and estrogen-induced kidney carcinogenesis in hamsters. Environ Health Perspect 105:565–569

Lyons WR (1958) Hormonal synergism in mammary growth. Proc R Soc Lond B Biol Sci 149:303–325

Macias H, Hinck L (2012) Mammary gland development. Wiley Interdiscip Rev Dev Biol 1(4):533–557

Mallepell S, Krust A, Chambon P, Brisken C (2006) Paracrine signaling through the epithelial estrogen receptor α is required for proliferation and morphogenesis in the mammary gland. Proc Natl Acad Sci USA 103:2196–2201

McClellan HL, Miller SJ, Hartmann PE (2008) Evolution of lactation: nutrition v. protection with special reference to five mammalian species. Nutr Res Rev 21:97–116

Mulac-Jericevic B, Lydon JP, DeMayo FJ, Conneely OM (2003) Defective mammary gland morphogenesis in mice lacking the progesterone receptor B isoform. Proc Natl Acad Sci USA 100:9744–9749

Nandi S (1958) Endocrine control of mammary-gland development and function in the C3H/He Crgl mouse. J Natl Cancer Inst 21(6): 1039–1063

Oftedal OT (2002) The mammary gland and its origin during synapsid evolution. J Mammary Gland Biol Neoplasia 7: 225–252

Ormandy CJ, Camus A, Barra J, Damotte D, Lucas B, Buteau H, Brousse N, Babinet C, Binart N, Kelly PA (1997) Null mutation of the prolactin receptor gene produces multiple reproductive defects in the mouse. Genes Dev 11:167–178

Palmieri C, Saji S, Sakaguchi H, Cheng G, Sunters A, O'Hare MJ, Warner M, Gustafsson JA, Coombes RC, Lam EW (2004) The expression of oestrogen receptor (ER)-beta and its variants, but not ERalpha, in adult human mammary fibroblasts. J Mol Endocrinol 33:35–50

Parmar H, Cunha GR (2004) Epithelial-stromal interactions in the mouse and human mammary gland in vivo. Endocr Relat Cancer 11:437–458

Porter KB, Tsibris JC, Nicosia SV, Murphy JM, O'Brien WF, Rao PS, Spellacy WN (1995) Estrogen-lnduced Guinea Pig model for Uterine Leiomyomas: do the ovaries protect? Biol Reprod 52:824–832

Richert MM, Schwertfeger KL, Ryder JW, Anderson SM (2000) An atlas of mouse mammary gland development. J Mammary Gland Biol Neoplasia 5:227–241

Roberts CM, Weir BJ (1973) Implantation in the plains viscacha, *Lagostomus maximus*. J Reprod Fertil 33:299–307

Russo J, Russo IH (1987) Development of the human mammary gland. In: Neville MC, Daniel CW (eds) The mammary gland. Development, regulation and function. Plenum Publishing, New York, pp 67–93

Russo H, Russo J (1996) Mammary Gland Neoplasia in long-term rodent studies. Environ Heah Perspm 104:938–967

Sakakura T (1987) Mammary embryogenesis. In: Neville MC, Daniel CW (eds) The mammary gland. Development, regulation and function. Plenum Publishing, New York, pp 37–66

Schedin P, Hovey RC (2010) The mammary stroma in normal development and function. J Mammary Gland Biol Neoplasia 15:275–277

Shyamala G, Yang X, Cardiff RD, Dale E (2000) Impact of progesterone receptor on cell-fate decisions during mammary gland development. Proc Natl Acad Sci USA 97:3044–3049

Sternlicht MD (2006) Key stages in mammary gland development. The cues that regulate ductal branching morphogenesis. Breast Cancer Res 8:201

Tingen C, Kim A, Woodruff TK (2009) The primordial pool of follicles and nest breakdown in mammalian ovaries. Mol Hum Reprod 15:795–803

Vonderhaar BK (1988) Regulation of development of the normal mammary gland by hormones and growth factors. In: Lippman ME, Dickson RB (eds) Breast cancer: cellular and molecular biology. Kluwer, Boston, pp 251–266

Watson CJ (2006) Key stages in mammary gland development. Involution: apoptosis and tissue remodelling that convert the mammary gland from milk factory to a quiescent organ. Breast Cancer Res 8:203

Watson CJ, Khaled WT (2008) Mammary development in the embryo and adult: a journey of morphogenesis and commitment. Development 135:995–1003

Weir BJ (1971a) The reproductive physiology of the plains viscacha, *Lagostomus maximus*. J Reprod Fertil 25:355–363

Weir BJ (1971b) The reproductive organs of the female plains viscacha, *Lagostomus maximus*. J Reprod Fertil 25:365–373